Synthesis and Characterization of Glutaraldehyde-Crosslinked Calcium Alginate for Fluoride Removal from Aqueous Solutions

Y. Vijaya,[1] Srinivasa R. Popuri,[2] A. Subba Reddy,[1] A. Krishnaiah[1]

[1]*Biopolymers and Thermophysical Laboratory, Department of Chemistry, Sri Venkateswara University, Tirupati 517502*
[2]*Department of Biological and Chemical Sciences, The University of the West Indies, Cave Hill, Barbados 11000*

Received 13 May 2009; accepted 11 September 2010
DOI 10.1002/app.33375
Published online 14 February 2011 in Wiley Online Library (wileyonlinelibrary.com).

ABSTRACT: A novel biosorbent was developed by the crosslinking of an anionic biopolymer, calcium alginate, with glutaraldehyde. The glutaraldehyde-crosslinked calcium alginate (GCA) was characterized by Fourier transform infrared spectroscopy and porosity and surface area analysis. The batch equilibrium and column flow adsorption characteristics of fluoride onto the biosorbent were studied. The effects of the pH, agitation time, concentration of adsorbate, and amount of adsorbent on the extent of adsorption were investigated. The experimental data were fitted to the Langmuir and Freundlich adsorption isotherms. The data were analyzed on the basis of the Lagergren pseudo-first-order, pseudo-second-order, and Weber–Morris intraparticle diffusion models. The maximum monolayer adsorption capacity of the GCA sorbent as obtained from the Langmuir adsorption isotherm was found to be 73.5 mg/g for fluoride. The χ^2 and sum of squares of the error analysis were used to correlate the equilibrium isotherm models and kinetics. In addition, breakthrough curves were obtained from column flow experiments. The experimental results demonstrate that the GCA beads could be used for the defluoridation of drinking water through adsorption.
 J Appl Polym Sci 120: 3443–3452, 2011

Key words: adsorption; biopolymers; FT-IR; kinetics (polym.); modeling

INTRODUCTION

In recent times, much public attention has been drawn to the fluoride content in drinking water. Fluoride is added to drinking water in small quantities to prevent dental caries. On the other hand, fluoride is a bone seeker and is linked to hip fractures and brittle bones.[1] Fluoride normally enters the environment and human body through water, food, industrial exposure, drugs, cosmetics, and so on. However, drinking water is the single major source of daily intake.[2] The World Health Organization[3] has specified the tolerance limit of the fluoride content of drinking water as 1.5 mg/L. The presence of a large amount of fluoride induces dental and skeletal fluorosis and nonskeletal fluorosis. The only option for preventing and controlling fluorosis is the defluoridation of drinking water. Various methods have been suggested for reducing the fluoride concentration in drinking water, namely, adsorption[4] precipitation,[5] ion exchange,[6] reverse osmosis,[7] nanofiltration,[8] electrodialysis,[9] and Donnan dialysis.[10] Each of these techniques has advantages and disadvantages that limit its use. For example, trivalent metals, such as aluminum, iron, and lanthanum, and divalent metals, such as calcium and magnesium, have been widely used to precipitate fluoride and arsenic in water streams.[11–14] The negatively charged fluoride ion is highly attracted to positively charged ions, such as calcium ions. Theoretically, the adsorption of fluoride onto solid particles normally takes three essential steps:[15] (1) the diffusion or transport of fluoride ions to the external surface of the adsorbent from the bulk solution across the boundary layer surrounding the adsorbent particle, (2) the adsorption of fluoride ions onto particle surfaces, and (3) the adsorbed fluoride ions probable exchange with the structural elements inside the adsorbent particles; this depends on the chemistry of solids or whether the adsorbed fluoride ions are transferred to the internal surfaces for porous materials (intra particle diffusion). The adsorption capacity also strongly depends on the pH, and its charges are generally positive under acidic conditions and negative in an alkaline environment. In general, the more positive the surface is, the better the sorption will be for negatively charged ions, such

Correspondence to: A. Krishnaiah (abburikrishnaiah@gmail.com).

as fluoride. It was reported in the literature that the presence of chemical functional groups, such as hydroxyl, carbonyl, carboxyl, sulfhydryl, theioether, sulfonate, amine amide, imidazole, phosphonate, and phosphodiester groups, present on the biosorbent surface contribute to biosorption.[16–19]

Among these methods reported, adsorption is one of the widely used methods for fluoride removal because of its ease of operation and cost effectiveness. The efficiency of the adsorption technique depends on the nature of the adsorbents used. Many adsorbents have been tried for fluoride removal, namely, hydrated cement,[20] hydroxyapatite,[21] activated carbon,[22,23] quick lime,[24] hydrotalcite,[25] clay,[26,27] ion exchangers,[28] cotton cellulose,[29] waste residue,[30] plaster of paris,[31] brick powder,[32] schwertmannite,[33] composite,[34] and so on.

Because environmental protection is becoming an important global problem, biosorption has become a promising technique for removing toxic ions.[35] Alginate is a family of polysaccharides composed of α-L-glucoronic acid (G) and β-D-mannuric acid (M) residues arranged in homopolymeric blocks of each type (MM GG) and in heteropolymeric blocks (MG). These are known to be hemocompatible and do not accumulate in any organs of the human body. When sodium is replaced by calcium in sodium alginate, each calcium ion coordinates to two alginate chains, linking them together. The flexible chains then become less flexible and form a huge network. The alginate molecule contains loads of hydroxyl groups (OHs), which can be coordinated to calcium ions.

The primary objective of this research was to study the biosorption of fluoride from an aqueous environment by glutaraldehyde-crosslinked calcium alginate (GCA) under equilibrium and column flow conditions. The secondary objective was to investigate the effects of the pH, contact time, concentration of fluoride, and amount of biosorbent on the extent of adsorption. The tertiary objective included the fitting of the experimental data to the Freundlich and Langmuir adsorption isotherms and Lagergren first-order, pseudo-second-order, and Weber–Morris intraparticle diffusion kinetic models.

EXPERIMENTAL

Chemicals

Sodium alginate, used to prepare the calcium alginate (CA) beads, was obtained from Loba Chemie (Mumbai, India). Glutaraldehyde, used to crosslink the CA beads, was obtained from Ranboxy Fine Chemicals (New Delhi, India). Analytical-reagent-grade sodium fluoride, hydrochloric acid, and sodium hydroxide from S. D. Fine Chemicals (Mumbai, India) were used as sources of fluoride and for the pH adjustment. Total ionic strength adjustment buffer was used to eliminate the interference effect of complexing ions from fluoride solution and was obtained from Thermo Electron Corporation, Waltham, Massachusetts, USA.

A stock solution of fluoride was prepared by the dissolution of 2.21 g of sodium fluoride in 1000 mL of double-distilled water such that each milliliter of the solution contained 1 mg of fluoride. The exact concentration of fluoride solution was calculated on a mass basis and is expressed in terms of milligrams per liter. The required lower concentrations were prepared by the dilution of the stock solution. All precautions were taken to minimize the loss due to evaporation during the preparation of the solutions and subsequent measurements. The stock solutions were freshly prepared for each experiment as the concentration of the stock solution could change on long standing.

Preparation of GCA beads

The sodium alginate solution was prepared by the dissolution and gentle heating of 40 g of alginate in 960 mL of water. The solution was then poured into a 2% calcium chloride solution through the tip of the transfer pipette. The drops of sodium alginate solution gelled into an average size of 3.5 ± 0.1 mm diameter beads upon contact with the calcium chloride solution. The beads were kept in contact with the calcium chloride solution for 4 h; this lead to the formation of insoluble and stable beads. Water-soluble sodium alginate was converted to water-insoluble CA beads with a $CaCl_2$ solution. The beads were rinsed with double-distilled water and dried until the water was completely evaporated. The size of the beads decreased on drying. Fine beads of the completely dried sample were taken randomly, and the size of the each bead was measured with a micrometer screw gauge with an accuracy of ±0.01 mm. The average size of the bead was found to be 2.05 mm.

Thirty grams of prepared CA beads were soaked in 250 mL of 0.01*M* glutaraldehyde, and the chemical reaction between the hydroxyl groups of CA and glutaraldehyde was confirmed by Fourier transform infrared (FTIR) measurements. The beads thus formed were dried and used in the fluoride removal from the aqueous medium.

FTIR spectral and surface area analysis

FTIR spectra of the biosorbent before and after the adsorption of fluoride were recorded in the frequency range 400–4000 cm^{-1} with an FTIR spectrophotometer (PerkinElmer-283B, Waltham, Massachusetts, USA). The sample (0.5 g) was formed into

pellets with KBr (0.5 g). The surface area of the GCA beads were measured by the single-point Brunauer–Emmett–Teller method with a thermal conductivity detector (Carlo Erba Soptomatic-1800, Milan, Italy) within the range 0.1–118.34 m^2/g with a sample size of 2.05 mm. The Pycnomatic ATC (automatic temperature controller) was uniquely designed for the density measurement of solid and powder samples. *Porosity* is defined as the fraction of apparent volume of the adsorbent that is attributed to the pores detected. The pore volume, density, and porosity of the biosorbent samples were measured with a Pycnomatic ATC (Thermo Electron S.P.A., Milan, Italy).

Equilibrium studies

Fluoride stock solutions were diluted to required concentrations for obtaining solutions containing 10, 15, and 25 mg/L of fluoride. Batch experimental studies were carried out with known weights of adsorbent and 100 mL of fluoride solution of a desired concentration at an optimum pH in 125-mL Erlenmeyer flasks. The flasks were agitated on a mechanical shaker (Ashok United Scientific Co., Chennai, India) at 200 rpm for a known period of time at room temperature. After equilibrium was obtained, the adsorbent was separated by filtration with Whatman No.41 filter paper manufacturer (Whatman plc, Maidstone, Kent, UK), and the aqueous-phase concentration of fluoride was determined with an ion-selective electrode (Orion 94-09, Thermo Fisher Scientific Inc, Waltham, Massachusetts, USA.). The equilibrium uptake capacity of the biosorbent for fluoride was calculated according to mass balance:

$$q_e = \left(\frac{C_i - C_e}{m}\right) \times v \quad (1)$$

where q_e is the amount adsorbed per unit mass of adsorbent (mg/g); C_i and C_e are the initial and equilibrium concentrations of fluoride (mg/L), respectively; m is the mass of adsorbent (g); and v is the volume of solution (L). Control experiments were conducted with fluoride solutions in the absence of biosorbent, and we found no fluoride adsorption by the walls of the container. We studied the effect of the pH of the medium on fluoride removal by performing equilibrium sorption experiments at different pH values. A pH meter Elico Limited (Hyderabad, India) with a combined glass electrode was used for pH measurements. The adjustment of the pH was made with 0.1*M* HCl and 0.1*M* NaOH solutions. We studied the effect of pH by keeping the fluoride concentration, amount of biosorbent, contact time, and temperature constant.

TABLE I
Surface Properties of GCA

Sample	Property	GCA
1	Surface area (m^2/g)	118.34
2	Porosity (%)	45.31
3	Pore volume (cm^3/g)	0.53
4	Pore diameter (cm/g)	0.85
5	Density (g/cm^3)	3.34
6	Ion-exchange capacity (mequiv/g)	0.98

Column adsorption and desorption experiments

Column flow adsorption experiments were conducted in a glass column of about 1.5-cm internal diameter and 10-cm length. The column was packed with the adsorbent while the column was shaken so that maximum amount of adsorbent was packed without gaps. A constant flow rate (2 mL/min) was maintained throughout the experiment with a peristaltic pump (model 7518-10, Cole Parmer, Illinois, USA). The effluent solution was collected at different time intervals, and the concentration of the fluoride in the effluent solution was monitored by an ion-selective electrode. The solutions were diluted appropriately before analysis. We obtained breakthrough curves for the adsorption of fluoride on the biosorbent by plotting the volume of the solution against the ratio of the concentrations of fluoride in the effluent and in the influent solutions (C_e/C_i).

After the column was exhausted, we drained the remaining aqueous solution off of the column by pumping air. The desorption of solutes from the loaded adsorbent was carried out by the solvent elution method with 0.05*M* ethylene diamine tetraacetic acid (EDTA) as an eluent. Then, EDTA solution was pumped into the column and maintained at constant temperature at a fixed flow rate of 0.5 mL/min. From the start of the experiment, effluent samples at different time intervals were collected at the bottom of the column for analysis. After regeneration, the adsorbent column was washed with distilled water to remove EDTA from the column before the influent fluoride solution was reintroduced for the subsequent adsorption–desorption cycle. Thus, the adsorption–desorption cycles were performed three times with the same bed to check the sustainability of the bed for repeated use.

RESULTS AND DISCUSSION

Characterization of the biosorbent

We understood from the data in Table I that the internal pores of the GCA beads had a small volume, which may have been surrounded by void particles; nevertheless, they contributed to much of the adsorption of the fluoride ions. It is a well-known

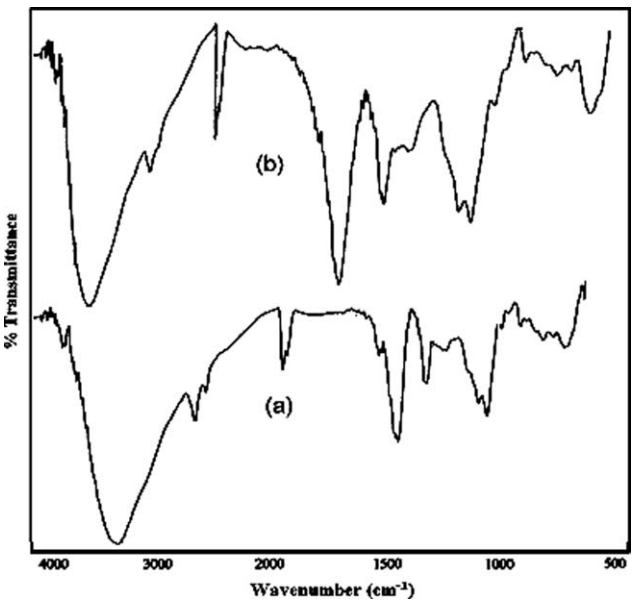

Figure 1 FTIR spectra of (a) GCA and (b) GCA with fluoride.

fact that the pore structure of plant and animal tissues, which are of vital importance, are formed fulfilling stringent conditions determined by the natural processes of cell division, self-organization, and so on, whose processes are yet to be understood clearly. GCA showed a higher percentage porosity, which meant that the higher pore volume and greater number of pores was available for the adsorption of fluoride ions. Thus, the porosity is one of the characteristics that determine the strength of the adsorbent to adsorb the fluoride ions from the liquids.

The characteristic patterns of the FTIR spectra of GCA (before and after fluoride adsorption) are shown in Figure 1. In the FTIR spectrum of the GCA adsorbent, there were adsorption bands at 2936 and 2871 cm^{-1}, which were assigned to the —CH2— and C—H stretching of aliphatic —CH_2 groups, respectively. C—H bending vibration was observed in the 1463–468-cm^{-1} spectral region. A broad band between 3134 and 3672 cm^{-1} corresponded to the O—H stretching mode. The O—H bonding vibration was observed as a weak band close to 1660 cm^{-1}. However, the alginic acid had a strong band of characteristic absorption at 1740 cm^{-1}; this might have been indicative of the free carboxyl group of the alginic acid of GCA, whereas the bands at 1630 and 1425 cm^{-1} were assigned to the presence of the carboxyl group [Fig. 1(a)]. The bands at 1630 and 1425 cm^{-1} were assigned to the antisymmertic and symmetric COO— stretching vibrations, respectively, of the carboxyl groups present in the alginates.[36,37] There was a reduction in the intensity of —OH bands at 3570 and 630 cm^{-1} with some displacement to lower frequencies in the fluoride-treated GCA; this may have been due to fluoride adsorption. The appearance of a new band at 745 cm^{-1} in the fluoride-treated GCA [Fig. 1(b)] confirmed the formation of the O—Ḣ—F bond. The characteristic band of C—F was observed as a small and broad band at 1014 cm^{-1} in the fluoride-loaded GCA biosorbent, whereas the same band was absent in the unloaded beads. Fluoride removal by the GCA sorbent was mainly governed by an electrostatic adsorption mechanism. The positively charged Ca^{+2} at the surface of the alginate attracted negatively charged fluoride ions by means of electrostatic attraction.

Scanning electron microscopy (SEM), recorded with a software-controlled digital scanning electron microscope, are given in Figure 2. The SEM clearly revealed the surface texture and morphology of the biosorbent. It was evident from the SEM micrographs that the GCA beads before fluoride adsorption showed a more uniform and homogeneous distribution of pores on the surface, as shown in Figure 2(a), but on fluoride loading, the biosorbent

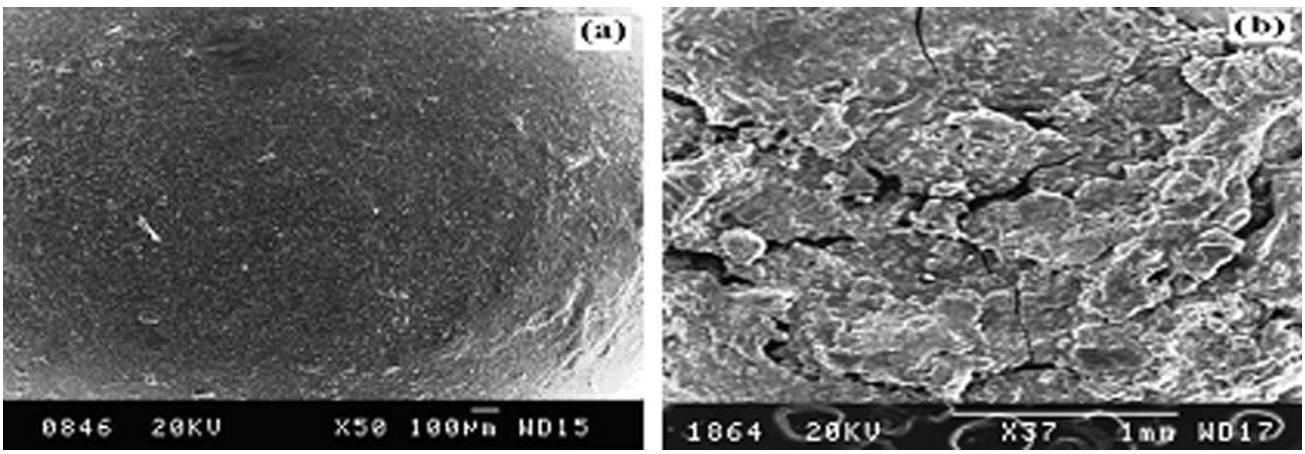

Figure 2 SEM images were recorded at Indian Institute of Science (IISc), Banglore, India (a) GCA and (b) GCA with fluoride.

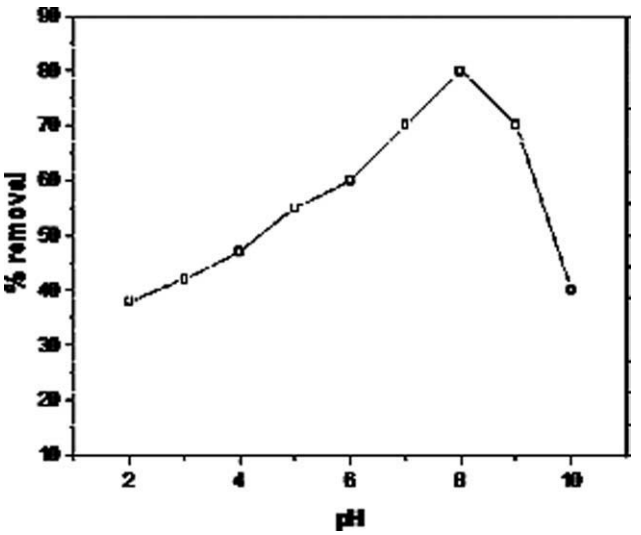

Figure 3 Effect of the pH on the percentage removal of fluoride on GCA.

surface showed no particular shape or crystalline structure, and it appeared rather like flakes, and the biosorbent became more brittle, as shown in Figure 2(b). The surface morphology and texture of fluoride-loaded biosorbent were completely different from the fluoride-unloaded biosorbent. There was a change in the morphology of the biosorbents after fluoride sorption. Surface morphological studies revealed that the process of fluoride sorption on the GCA beads was predominantly a surface phenomenon.

Effect of the pH

The pH of the medium is one of the important parameters that significantly affect the extent of fluoride adsorption. Fluoride removal by the adsorbent was studied over the pH range 2–10 with an adsorbent dose of 0.5 g/100 mL, an initial concentration of 10 mg/L, a shaking speed of 200 rpm, and a contact time of 120 min. As the pH of the fluoride solution increased from 2 to 10, the adsorption capacity of fluoride was changed; it first increased to 1.6 mg/g (80%) at pH 8 and then slightly decreased to 1.4 mg/g (70%) at pH 9. After that, the adsorption capacity dramatically decreased, and the adsorbent exhibited negligible adsorption [0.8 mg/g (40%)] at pH 10, as shown in Figure 3. The quick reduction of the amount of fluoride adsorbed in the alkaline pH range was attributed to the competition of hydroxyl ions with fluoride for adsorption sites.[38] The relatively lower adsorption of fluoride in the acidic range (pH < 5) may have been due to the formation of weakly ionized hydrofluoric acid.[39] It is important to mention here that the optimized pH was 8. pH_{zpc} = pH at the zero point of charge (zpc) is an indicator of the net surface charge of the adsorbent and its preference for ionic species. At pH < $pH_{zpc,}$ the surface charge is positive, at pH = pH_{zpc}, the surface charge is neutral, and at pH > pH_{zpc}, the surface charge is negative. The pH_{zpc} value of GCA was found to be 7.8. Chemisorption occurred below the pH_{zpc} value and above the pH_{zpc} value; this suggested that sorption was mainly due to physisorption.

Adsorption isotherms

The analysis of adsorption data is important for developing an equation that accurately represents the results and that could be used for design purposes. The most commonly applied isotherms in solid/liquid systems are the theoretical isotherms, Langmuir and Freundlich. In this study, we attempted to analyze adsorption at different concentrations (10–60 mg/L) by these two models. The linear regression was used to determine the most fitted model among two adsorption isotherms. The most widely used isotherm equation for modeling equilibrium is the Langmuir equation[40]:

$$Q_e = \frac{Q^o b C_e}{1 + bC_e} \tag{2}$$

where Q_e is the amount of fluoride adsorbed per unit weight of the sorbent (mg/g) and Q^o and b are Langmuir constants indicating the adsorption capacity and energy of adsorption, respectively. The linear plot of $1/C_e$ versus $1/Q_e$, with high correlation coefficient (r^2) values, indicated the monolayer adsorption on GCA. The values of Q^o and b were determined from linear plots and are presented in Table II. The adsorptive capacity of GCA to remove fluoride was compared with those of other adsorbents reported in the literature (Table III).

To determine the feasibility of the isotherm, the essential characteristics of the Langmuir isotherm

TABLE II
Langmuir and Freundlich Isotherm Parameters with χ^2 Analysis of Fluoride Sorption on GCA

Langmuir isotherm parameters				Freundlich isotherm parameters				
Q^o (mg/g)	b (L/mg)	r^2	χ^2	K_f (mg/g)	$1/n$ (L/mg)	n	r^2	χ^2
73.5	0.006	0.997	58.22	0.496	0.932	1.073	0.989	116.57

TABLE III
Comparison of the Data of Fluoride Sorption Capacity with GCA with Published Data

Adsorbent	Q^o (mg/g)	Reference
Hydrated cement	2.6788	20
Synthetic hydroxyapatite	3.113	21
Modified activated carbon	23.3	22
Quicklime	16.67	24
Ion exchanger	90.0	28
Cotton cellulose	21.05	29
Plaster of paris	0.283	31
Brick powder	41.56	32
Schwertmannite	33.3	33
GCA	73.5	This study

can be expressed in terms of the dimensionless constant separation factor (R_L)[41,42]:

$$R_L = \frac{1}{1 + bC_i} \tag{3}$$

A value of R_L of less than 1.0 represents favorable adsorption, and a value greater than 1.0 represents unfavorable adsorption. The values of R_L for the sorption of fluoride on GCA were less than 1 and greater than 0; this indicated favorable uptake of fluoride by the biosorbent.

The Freundlich[43] equation is commonly used to explain adsorption data. This model assumes that uptake of fluoride ions occurs on the heterogeneous adsorbent surface. The Freundlich equation is expressed as follows:

$$Q_e = K_f C_e^{1/n} \tag{4}$$

where K_f is a measure of the adsorption capacity and $1/n$ is the adsorption intensity, evaluated from the plot of log Q_e versus log C_e. The values of the Freundlich parameters K_f and n along with r^2 are presented in Table II. The values of $1/n$ were between 0.1 and 1.0; this confirmed the favorable conditions for adsorption.[44]

χ^2 analysis

To identify a suitable isotherm model for the sorption of fluoride on GCA, this analysis was carried out. The χ^2 test statistic is basically the sum of the squares of the differences between the experimental data and the data obtained by calculation from models, with each squared difference divided by the corresponding data obtained by calculation from the models. The equivalent mathematical statement is

$$\chi^2 = \sum \left[\frac{(q_e - q_{e,m})^2}{q_{e,m}} \right] \tag{5}$$

where $q_{e,m}$ is the equilibrium capacity obtained by calculation from the model (mg/g) and q_e is the experimental data of the equilibrium capacity (mg/g). If the data from the model are similar to the experimental data, χ^2 will be a small number, whereas if they differ, χ^2 will be a bigger number. Therefore, it was also necessary to analyze the data set with the nonlinear χ^2 test to confirm the best-fit isotherm for the sorption system.[35] The χ^2 values were calculated and are given in Table II. The χ^2 values of both isotherms were comparable, and hence, the adsorption of fluoride on GCA followed both the Freundlich and Langmuir isotherms and fit better with the Langmuir isotherm as its χ^2 value was less than that of the Freundlich model.

Effect of the contact time

The effect of the contact time on the extent of adsorption of fluoride at different concentrations is shown in Figure 4. The extent of adsorption increased with time and attained equilibrium for all the concentrations of fluoride studied (10, 15, and 20 mg/L) at 90 min. The rate of uptake was rapid in the early stages, gradually decreased, and became constant when equilibrium was attained.[45] After this equilibrium period, the amount of fluoride adsorbed did not change significantly with time. This result was important for consideration of the treatment of wastewater and other similar applications.[46] The curves of the amount of fluoride adsorbed versus time were smooth and continuous. The changes in the rate of removal might be have been due to the fact that, initially, all adsorbent sites were vacant and the solute concentration gradient was high. Later, the fluoride uptake rate by adsorbent decreased significantly because of the decrease in the number of adsorption sites. A decreased removal

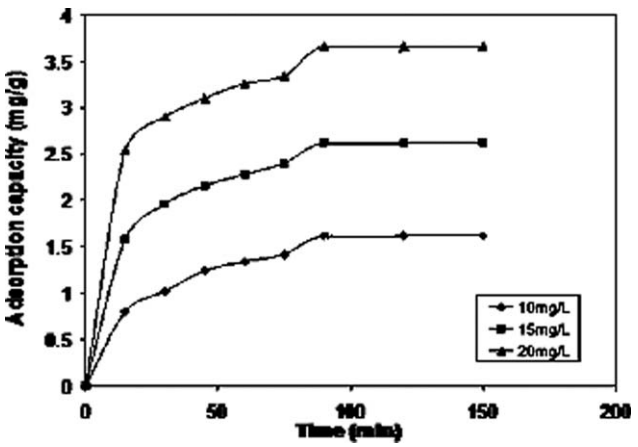

Figure 4 Effect of the time on the sorption of fluoride on GCA.

TABLE IV
Lagergren First-Order and Pseudo-Second-Order Kinetic Models of Fluoride Sorption on GCAs

Concentration of fluoride solution (mg/L)	First-order model		Second-order model			
	k_{ad}	r^2	$Q_{e\ found}$ (mg/g)	$Q_{e\ calcd}$ (mg/g)	k_2	r^2
10	0.024	0.996	1.62	1.906	0.023	0.994
15	0.025	0.996	2.62	2.894	0.025	0.997
20	0.021	0.993	3.66	3.940	0.024	0.997

rate, particularly toward the end of the experiment, indicated the possible monolayer of fluoride ions on the outer surface, pores of both the adsorbents, and pore diffusion onto the inner surface of the adsorbent particles through the film due to the continuous shaking maintained during the experiment.

Sorption dynamics

To investigate the mechanism of sorption, the rate constants of the sorption process were determined with the Lagergren first-order[47] and pseudo-second-order[48] kinetic models and were represented as follows:

$$\log(q_e - q_t) = \log q_e - \frac{k_{ad}}{2.303}t \tag{6}$$

$$\frac{t}{q_t} = \frac{1}{k_2 q_e^2} + \frac{1}{q_e}t \tag{7}$$

where q_e and q_t (mg/g) are the amounts of the fluoride ions sorbed at equilibrium (mg/g) and at time t (min), respectively, and k_{ad} (min^{-1}) and k_2 (g mg^{-1} min^{-1}) are the rate constants. The values of the first- and second-order rate constants are included in Table IV for initial concentrations of 10, 15, and 20 mg/L, respectively. In many cases, the first-order equation of Legergren did not fit well to the whole range of contact time and was generally applicable over the initial stage of the adsorption process.[49] The second-order kinetic model assumes that the rate-limiting step may be chemical adsorption.[50] In many cases, the adsorption data could be well correlated by a second-order rate equation over the entire period of contact time.[51] The results of this study indicate that the adsorption of fluoride on GCA followed second-order kinetics. The r^2 values for this model were nearer to unity compared to the r^2 values obtained in first-order kinetics.[52]

TABLE V
SSE Values of the Kinetic Models Used for the Fluoride Sorption on GCA

Model	10 mg/L	15 mg/L	20 mg/L
First-order model	1.572	2.570	3.618
Second-order model	0.050	0.028	0.021

Fitness of the sorption kinetic models

The assessment of the kinetic models that we used for fitting the sorption data was made by calculation of the sum of squares of the error (SSE). Lower values of SSE showed better fit to the sorption data and gave an indication of the sorption mechanism:

$$\mathrm{SSE} = \sum \frac{(q_{t,e} - q_{t,m})^2}{q_{t,e}^2} \tag{8}$$

where $q_{t,e}$ and $q_{t,m}$ are the experimental sorption capacity of fluoride (mg/g) at time t and the corresponding value that is obtained from the kinetic models, respectively. SSE values of the Lagergren first- and pseudo-second-order kinetic models were computed and are summarized in Table V. We assumed that the model that gave the lowest SSE values was the best model for this system, and then, the mechanism of sorption could be explained on the basis of that model. As shown in Table V, the pseudo second-order model seemed to fit better than the pseudo-first-order model for representing the kinetics of fluoride sorption.

Effect of the adsorbent dose

The effect of the adsorbent dose on the removal of fluoride at optimum pH (8) is shown in Figure 5.

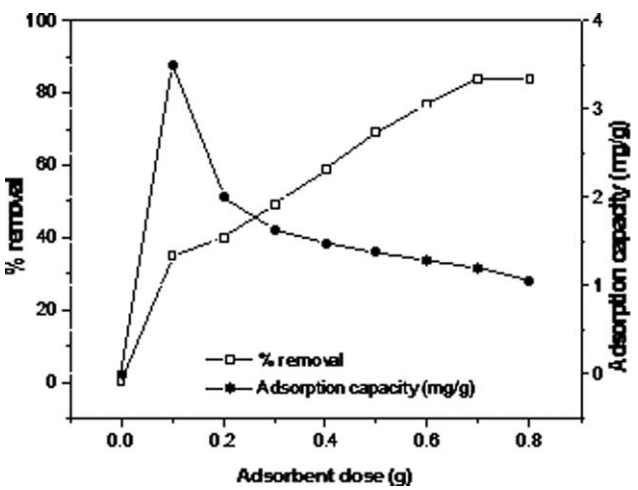

Figure 5 Effect of the adsorbent dose on the percentage removal of fluoride on GCA.

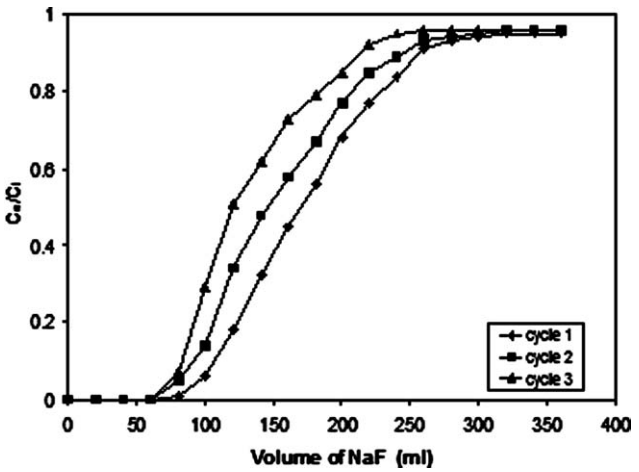

Figure 6 Column breakthrough curves for the sorption of fluoride on GCA.

The amount of adsorbent significantly influenced the extent of fluoride adsorption. The extent of fluoride removal was 35% (3.5 mg/g) with a 0.10 g/0.1 L adsorbent dose, whereas it was greatly increased to 77% (1.28 mg/g) with a 0.6 g/0.1 L adsorbent dose. However, when the adsorbent was about 0.7 g/0.1 L, the percentage removal increased to 84% (1.2 mg/g) only. Furthermore, a higher adsorbent dose results in lower q_e (mg/g) values at a fixed fluoride concentration (10 mg/L), as shown in Figure 5. The decrease in the adsorption capacity with increasing adsorbent dose was mainly due to the unsaturation of adsorption sites through the adsorption process.[53]

Column adsorption studies

Fluoride biosorption dynamics in a fixed-bed flow through a sorption column was eventually conducted for multiple reuse of the biosorbent. Column adsorption studies of fluoride on the GCA beads at room temperature were investigated with an aqueous solution at 10 mg/L influent concentrations (C_i's), at the optimal pH value of 8. We obtained experimental breakthrough curves by plotting a graph between the ratios of the effluent concentration to initial concentration versus the volume of the effluent, as shown in Figure 6. The measurement of the sorbent mass was more precise than the determination of the respective volume. Therefore, the sorbent quantity was used preferably instead of the bed height.[54] We obtained the data by passing the fluoride solution through a bed packed with dried GCA beads in a downward flow at a rate of 2 mL/min and determining the concentration of fluoride ions at different time intervals in the effluent solution. When the column was saturated, it was regenerated and subsequently used for the next adsorption process.

Breakthrough is supposed to be attained when the concentration of solute in the effluent is equal to the influent concentration and remains unchanged thereon.[55] Faster and more effective adsorption of fluoride occurred during the initial phase. Subsequent fluoride adsorption decreased as a consequence of the progressive saturation of the binding sites. It was observed that the column was saturated after we passed 320 mL of fluoride solution in the first cycle. The maximum breakthrough adsorption capacity of the biosorbents was observed in first cycle and subsequently decreased in the second and third cycles for GCA.

Desorption studies

When the bed was exhausted or the effluent coming out of the column reached the allowable maximum discharge level, the regeneration of the adsorption bed to recover the adsorbed material and/or to regenerate the adsorbent became quite essential. The regeneration could be accomplished by a variety of techniques, including thermal decomposition, steam washing, and solvent extraction. Each method has inherent advantages and limitations. In this study, several solvents were used to regenerate the adsorption bed. A 0.05*M* EDTA solution was found to be effective for desorbing and recovering fluoride ions quantitatively from the adsorption bed. EDTA was used as the solvent of choice because its solubility parameters and salvation forces of EDTA overweighed the attractive forces of GCA for fluoride ions. We regenerated the fixed-bed columns of the GCA beads saturated with fluoride by passing EDTA solution as an eluant at a fixed flow rate of 0.5 mL/min. To evaluate the fluoride recovery efficiency, the percentage of fluoride ions recovered

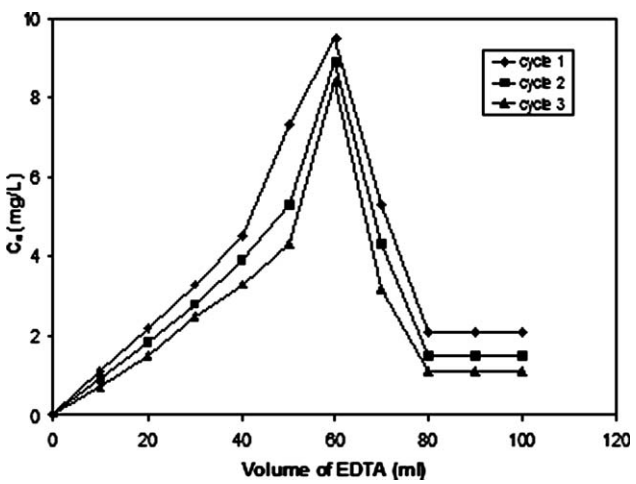

Figure 7 Desorption curves of the fluoride adsorbed on GCA.

was calculated from the breakthrough and recovery curves. More specifically, maximum desorption occurred at 60 mL of EDTA solution, and complete regeneration occurred at about 80 mL. These adsorption–desorption cycles were repeated three times. There was an early saturation of the bed with fluoride ions in the second and third cycles. The desorption profile is graphically presented in Figure 7. From the plots, we observed that the rate of desorption increased sharply and reached maximum with 60 mL of EDTA and decreased and attained a minimum with about 80 mL of EDTA solution. The regenerated column was further used for the removal of fluoride. The results indicate that the column was saturated early, and the adsorption capacity decreased slightly. As a result, the percentage desorption also decreased from the first cycle to the second cycle. Similar behavior was observed in the third cycle of the adsorption–desorption experiments.

CONCLUSIONS

In this study, GCA beads were successfully used as a biosorbing agent for the removal of fluoride ions from an aqueous solution. The maximum uptake of fluoride ions occurred at pH 8. An increase in the amount of biosorbent increased the percentage removal of fluoride ions. Furthermore, the biosorbent was characterized by surface area analysis, FTIR spectroscopy, and SEM techniques. The Langmuir and Freundlich adsorption models were used for the mathematical description of the biosorption of fluoride ions on to the GCA beads. The adsorption equilibrium data conformed well to the Langmuir model. The maximum biosorption capacities of the GCA beads in this study were 73.6 mg/g for fluoride. The kinetic studies indicated that the sorption of fluoride on GCA followed a pseudo-second-order model. This model seemed to fit better than the other two models (the pseudo-first-order and particle diffusion models) for representing the kinetics of fluoride sorption. Column adsorption and desorption experiments showed that it was possible to fully remove the fluoride ions bound with the adsorbent and regenerate the adsorbent.

References

1. Veressinina, Y.; Trapido, M.; Ahelik, V.; Munter, R. Proc Estonian Acad Sci Chem 2001, 50, 81.
2. Sarala, K.; Rao, P. R. Fluoride 1993, 26, 177.
3. Fluoride: Environmental Health Criteria; WHO Report; World Health Organization: Geneva, Switzerland, 1984.
4. Fink, G. J.; Lindsay, F. K. Ind Eng Chem 1936, 28, 947.
5. Parthasarathy, N.; Buffle, J.; Haerdi, W. Can J Chem 1986, 64, 24.
6. Popat, K. M.; Anand, P. S.; Dasare, B. D. React Polym 1994, 23, 23.
7. Joshi, S. V.; Mehta, S. H.; Rao, A. P.; Rao, A. V. Water Treat 1992, 7, 207.
8. Simons, R. Desalination 1993, 89, 325.
9. Adhikary, S. K.; Tipnis, U. K.; Harkare, W. P.; Govindan, K. P. Desalination 1989, 71, 301.
10. Hichour, M.; Persin, F.; Sandeaux, J.; Gavach, C. Sep Purif Technol 2000, 18, 1.
11. Nawlakhe, W. G.; Paramasivam, R. Curr Sci 1993, 65, 743.
12. Shen, F.; Chen, X.; Gao, P.; Chen, G. Chem Eng Sci 2003, 58, 987.
13. Vaaramaa, K.; Lehto, J. Desalination 2003, 155, 157.
14. Kang, M.; Chen, H.; Sato, Y.; Kamei, T.; Magara, Y. Water Res 2003, 37, 4599.
15. Fan, X.; Parker, D. J.; Smith, M. D. Water Res 2003, 37, 4929.
16. Crist, R. H.; Oberhulser, K.; Shanke, N.; Nguyen, M. Environ Sci Tech 1981, 15, 1212.
17. Greene, B.; McPherson, R.; Damall, D. Metals Speciation, Separation and Recovery; Lewis: Chelsea, MI, 1987; p 315.
18. Mann, H. Biosorption of Heavymetals; CRC: Boca Raton, FL, 1990; p 93.
19. Hunt, S. Immobilization of Ions by Biosorption; Ellis Harwood: Chichester, England, 1996; p 15.
20. Kagne, S.; Jagtap, S.; Dhawade, P.; Kamble, S. P.; Devotta, S.; Rayalu, S. S. J Hazard Mater 2008, 154, 88.
21. Sairam, S. C.; Viswanathan, N.; Meenakshi, S. J Hazard Mater 2008, 215, 206.
22. Daifullah, A. A. M.; Yakout, S. M.; Elreefy, S. A. J Hazard Mater 2007, 147, 633.
23. Mohan, D.; Singh, K. P.; Singh, V. K. J Hazard Mater 2008, 152, 1045.
24. Islam, M.; Patel, R. K. J Hazard Mater 2007, 143, 303.
25. Wang, H.; Chen, J.; Cai, Y.; Ji, J.; Liu, L.; Teng, H. H. Appl Clay Sci 2007, 35, 59.
26. Meenakshi, S.; Sairam, S. C.; Sukumar, R. J Hazard Mater 2008, 153, 164.
27. Tor, A. Desalination 2006, 201, 267.
28. Chubar, N. I.; Samanidou, V. F.; Kouts, V. S.; Gallios, G. G.; Kanibolotsky, V. A.; Strelko, V. V.; Zhuravlev, I. Z. J Colloid Interface Sci 2005, 291, 67.
29. Zhao, Y.; Li, X.; Liu, L.; Chen, F. Carbohydr Polym 2008, 72, 144.
30. Nigussie, W.; Zewge, F.; Chandravanshi, B. S. J Hazard Mater 2007, 147, 954.
31. Gopal, V.; Elango, K. P. J Hazard Mater 2007, 141, 98.
32. Yadav, A. K.; Kaushik, C. P.; Haritash, A. K.; Kansal, A.; Rani, N. J Hazard Mater 2006, 128, 289.
33. Eskandarpour, A.; Onyango, M. S.; Ochieng, A.; Asai, S. J Hazard Mater 2008, 152, 571.
34. Sairam, S. C.; Viswanathan, N.; Meenakshi, S. Bioresour Technol 2008, 99, 8226.
35. An, H. K.; Park, B. Y.; Kim, D. S. Water Res 2001, 35, 3551.
36. Rabek, J. F. Experimental Methods in Polymer Chemistry; Wiley: New York, 1980; p 238.
37. Huang, R. Y. M.; Pal, R.; Moon, G. Y. J Membr Sci 1999, 160, 101.
38. Raichur, A. M.; Basu, M. J. Sep Purif Technol 2001, 24, 121.
39. Sujana, M. G.; Thakur, R. S.; Rao, S. B. J Colloid Interface Sci 1988, 206, 94.
40. Langmuir, I. J Am Chem Soc 1916, 38, 2221.
41. Raji, C.; Anirudhan, T. S. Water Res 1998, 32, 3772.
42. McKay, G.; Blair, H. S.; Gardner, J. R. J Appl Polym Sci 1982, 27, 3043.
43. Freundlich, H. F. M. Z Phys Chem 1906, 57, 385.
44. Meenakshi, S.; Viswanathan, N. J Colloid Interface Sci 2007, 308, 438.
45. Sharma, Y. Colloid Surf A 2003, 55, 215.
46. Shakinah, P.; Kadirivelu, K.; Kanmani, P.; Subburam, V. J Chem Technol Biotechnol 2002, 77, 458.

47. Das, N.; Pattanaik, P.; Das, R. J Colloid Interface Sci 2005, 292, 1.
48. Quek, S. Y.; Wase, D. A. J.; Forster, C. F. Water SA 1998, 24, 251.
49. McKay, G.; Ho, Y. S. Water Res 1999, 33, 578.
50. Chiou, M. S.; Li, H. Y. J Hazard Mater 2002, 93, 233.
51. Sag, Y.; Aytay, Y. Process Biochem 1995, 30, 169.
52. Vijaya, Y.; Krishnaiah, A. E J Chem 2009, 6, 713.
53. Kovacevic, Z. F.; Sipos, L.; Briski, F. Food Technol Biotechnol 2000, 38, 211.
54. Hawari, H. A.; Mulligan, C. N. Process Biochem 2006, 41, 187.
55. Vijayaraghavan, K.; Jegan, J.; Palanivelu, K.; Velan, M. Chemosphere 2005, 60, 419.